Title

CHARACTERISTICS OF jt| PRODUCTION FROM PROTON-PROTON COLLISIONS NEAR THRESHOLD

Authors

Mover, Burton J.
Squire, Robert K.

Publication Date

1957-02-01

UCRL 3137 (Rev.)

UNIVERSITY OF CALIFORNIA

Radiation Laboratory

BERKELEY, CALIFORNIA

DISCLAIMER

UCRL-3137 (Rev.)

UNIVERSITY OF CALIFORNIA

Radiation Laboratory
Berkeley, California

Contract No. W-7405-eng-48

CHARACTERISTICS OF π^0 PRODUCTION FROM PROTON-PROTON COLLISIONS NEAR THRESHOLD

Burton J. Moyer and Robert K. Squire

February 1957

Printed for the U.S. Atomic Energy Commission

CHARACTERISTICS OF π^0 PRODUCTION FROM PROTON-PROTON COLLISIONS NEAR THRESHOLD

Burton J. Moyer and Robert K. Squire

Radiation Laboratory
University of California
Berkeley, California

February 1957

ABSTRACT

The angular distribution and excitation function for neutral mesons produced by proton-proton collisions near threshold have been measured. It is found that P-state production of the mesons dominates at all energies except those quite close to threshold, where some S-state production can be detected.

The total cross section, at an energy where the maximum attainable c.m. meson momentum is $\eta_0 M_\pi C$, can be stated as

$$\sigma(\text{mb}) = 0.02\ \eta_0^2 + 0.57\ \eta_0^8.$$

(S state) (P state)

CHARACTERISTICS OF π^0 PRODUCTION FROM PROTON-PROTON COLLISIONS NEAR THRESHOLD*

Burton J. Moyer and Robert K. Squire

Radiation Laboratory
University of California
Berkeley, California

February 1957

I. INTRODUCTION

It has been found possible to greatly simplify the analysis of the production of pions at low energies by applying various levels of phenomenological theories to the reactions in which they occur. In many cases this has amounted to no more than the application of some general quantum mechanical principles. In fact, by assuming that pions are produced chiefly in P states, and by treating the nucleon-nucleon interaction phenomenologically, it has been possible to explain the energy spectra and angular distribution of pions and in some cases to predict the excitation functions for the producing reactions.[1, 2]

One can make three major assumptions in the general analysis of pion-nucleon interactions.

1. Charge independence is valid.

2. The pion-nucleon interaction range is finite and is of the order of $\hbar/\mu C$.

3. A pion-nucleon system in the state $I = 3/2$, $J = 3/2$ has an especially strong (attractive) interaction.

---

*This work was done under the auspices of the U.S. Atomic Energy Commission.

[1] A. H. Rosenfeld, Phys. Rev. 96, 139 (1954).

[2] Gell-Mann and Watson, Annual Rev. Nucl. Sci. (Ann. Rev. Inc.) 4, 219 (1954).

In meson production by two colliding nucleons, at energies near threshold ($T_\pi < 60$ Mev), only the states of angular momentum equal to 0 or 1 will be important. We therefore have to consider that the meson may be in an S state or a P state with respect to the c.m. of the two-nucleon system, and these nucleons may be in an S or P state with respect to each other. For the nucleons, there is a strong tendency for the S state to predominate, with low nucleon energies in the final system.

If we list the reactions according to their (experimental) order of importance, we have:

Sp (nucleons in S final state, meson in P state),

Ss,

Pp,

Ps.

Brueckner and others have applied the above principles to the production of mesons from nucleon-nucleon collisions and have found it possible to express in terms of only three fundamental cross sections, the seven reactions that occur.[3, 4, 5] The excitation functions and angular distributions for these cross sections can be derived. If one adopts the notation of Rosenfeld,[1] in which $\sigma_{a,b}$ is the cross section for a reaction, then a is the initial isotopic spin and b the final isotopic spin of the two-nucleon system. In these terms, the three cross sections are σ_{10}, σ_{01}, and σ_{11}. The reaction $p + p \rightarrow \pi^0 + p + p$ involves the term σ_{11} only, and a study of it therefore should yield an unequivocal measure of this term.

---

[3] K. A. Brueckner, Phys. Rev. 82, 598 (1951).

[4] Chew, Goldberger, Steinberger, and Yang, Phys. Rev. 84, 58 (1951).

[5] K. M. Watson and K. A. Brueckner, Phys. Rev. 83, 1 (1951).

The following reactions occur.

π^0 Production by p-p collisions[1]

Class	Reactions	Angular distribution	Excitation function
Ss	$^3P_0 \rightarrow (^1S_0 s)_0$	isotropic	$\sim 0.01\ \eta_0^2$
Pp	$^3P_1 \rightarrow (^3P_0 p)_1$ $^3P_{0,\ 1,\ 2}$ or $^3F_2 \rightarrow (^3P_1 p)_{0,\ 1,\ 2}$ $^3P_{1,\ 2}$ or $^3F_{2,\ 3} \rightarrow (^3P_2 p)_{1,\ 2,\ 3}$	$\frac{c}{3} + \cos^2\theta$	$\sim 0.2\ \eta_0^8$
Ps	$^1S_0 \rightarrow (^3P_0 s)_0$ $^1D_2 \rightarrow (^3P_2 s)_2$	isotropic	$\propto \eta_0^6$
Sp	none	-	-

One can derive the excitation functions as follows:[2]

1. Class Ss

$$\frac{d\sigma_{11}}{dT_\pi} \propto \frac{\eta (T_0 - T)^{1/2}}{T_0 - T + B}\ ; \qquad [\sigma_{11}]_{Ss} \propto \eta_0^2,$$

2. Class Pp

$$\frac{d\sigma_{11}}{dT_\pi} \propto \eta^3 (T_0 - T)^{3/2}\ ; \qquad [\sigma_{11}]_{Pp} \propto \eta_0^8,$$

3. Class Ps

$$\frac{d\sigma_{11}}{dT_\pi} \propto \eta(T_0 - T)^{3/2}; \quad [\sigma_{11}]_{Ps} \propto \eta_0^6,$$

where η = meson momentum, units μc

η_0 = maximum meson momentum

T = nucleon energy

T_0 = total (c.m.) energy available

B = binding energy of the two nucleons in a (virtual) $^1S_0$ state, assumed to be small.

Previous experimental work thus far [6, 7, 8] has detected only the term $[\sigma_{11}]_{Pp}$ η_0^8. By carrying the measurements down to energies close to the threshold, one may hope to detect the other classes of production, and to therefore get a measure of the relative importance of the various production modes.

---

[6] J. Marshall and L. Marshall, Phys. Rev.

[7] J. W. Mather and E. A. Martinelli, Phys. Rev. 92, 780 (1953).

[8] R. A. Stallwood, "The Reaction p + p → π^0 + p + p in the Energy Region 346 Mev to 437 Mev," Report No. NYO-7108, March 1956, Carnegie Institute of Technology.

II. APPARATUS

A. Arrangement

The experiment was performed by allowing protons to pass through a liquid hydrogen target. The photons from the decay of the neutral mesons formed in the proton-proton collisions were detected by a gamma telescope.

The source of the protons was the 340-Mev Berkeley synchrocyclotron. The external beam from this machine was deflected by a steering magnet into the experimental area, where it was analyzed by a 12,000-gauss magnet, was deflected here by about 20°, passed through the target, and finally passed through an ionization chamber which served to measure the proton flux.

A counter array referred to below as a "telescope" was located to one side of the target, at a desired angle, and collimated so that it viewed only the region of intersection of the beam with the liquid hydrogen in the target.

The general layout is illustrated in Fig. 1, which also indicates the position of the pair of ion chambers used to measure the beam energy.

B. Beam

The proton beam emerging from the collimator is contaminated with neutrons. Deflecting the protons with a magnet made it possible to offset the target so that the neutrons were prevented from striking the target. The proton beam traversed the magnet without striking the pole tips or any other material, so as to avoid any further neutron production.

For maximum-energy protons, i.e., 340 Mev, it sufficies to use the beam as described above. To measure the excitation function, however, several energies are needed. These are achieved by introducing carbon absorbers in the path of the beam while it is still in the fringing field of the cyclotron. In this experiment, a rapid decrease in cross section with decreasing energy, coupled with a decrease in the beam intensity, made it impractical to work below 320 Mev.

The beam cross section was about 2 by 3 inches at the entrance to the target, and the target container was so constructed that at no point did the

protons come closer than 2 in. from the side walls or internal structures. This was done to insure that events really occurred in the liquid hydrogen only.

C. Target

The target was a volume of liquid hydrogen 6 by 22 by 14 in. Very little material could be tolerated in the beam path -- material on which protons could produce neutrons by charge-exchange scattering, or π^- mesons that could be captured in the liquid hydrogen. For these reasons we chose a double-walled Styrofoam target, as indicated in Fig. 2. The total amount of material traversed by the beam before entering liquid hydrogen was 0.175 g/cm^2.

The liquid depth was monitored by means of a float driving a light reed inside a graduated glass tube. After a few hours of operation, the rate of consumption of liquid hydrogen was found to be quite steady at about 4 liters per hour.

D. Monitor

The flux of protons was measured by allowing the beam to pass through a calibrated ionization chamber filled with helium gas. The beam size and shape were such that the entire beam passed through the sensitive region of the ion chamber.

E. Telescope

The detector was required to be an instrument with a high efficiency for detecting gamma rays in the presence of the very large background of radiation that one finds typical of the experimental "cave" area of the cyclotron.

In Fig. 3, the first unit is a plastic scintillator, somewhat larger in cross section than the following units, and designed to be 100% efficient for the detection of minimum-ionizing charged particles. This is called the "anti-scintillator," and is electronically placed in anticoincidence with the rest of the telescope. It rejects charged particles incident upon the array. This is followed by a lead sheet 2 by 2 by 0.206 in., which converts the gammas into electron-positron pairs. These emerge from the lead and pass successively

through a 1-in.-thick plastic scintillator, a 4-in. Cerenkov counter of lucite, and another 1-in. plastic scintillator. The two scintillators are placed in electronic coincidence and serve to state that a charged particle passed through them, and hence had an energy equal to or greater than that necessary to penetrate the intervening 4 in. of lucite. The Cerenkov counter served to identify the counting event as due to a charged particle having β approximately equal to 1. It was this counter which allowed discrimination between electrons and the very much more intense "background" of neutrons and stray radiation of other forms in the experimental area. The identification of a gamma consisted of simultaneous pulses in the two photomultipliers viewing scintillator No. 1 (Sc 1) and scintillator No. 2 (Sc 2) and in the two tubes viewing the Cerenkov radiation block, unaccompanied by a pulse from the "antiscintillator." The manifold-coincidence requirement was satisfactory in eliminating accidental counts.

F. Collimation

A collimator was constructed of lead bricks, which were machined for close fitting. It was 16 in. deep towards the target and contained a 2-by-2 in. hole aligned with the telescope. Enclosed by the lead was a block of beryllium, 2 by 2 by 8 in., which attenuated the flux of low-energy charged particles.

G. Electronics

The circuitry associated with the gamma telescope was composed of several fast-coincidence circuits, (5×10^{-9} sec) followed by slower amplifiers and mixing circuits (Fig. 4). Comprehensive descriptions of the fast electronics have been presented by Madey[9] and by Squire.[10] A gamma event was identified by a coincidence between Sc1 and Sc2, and Cerenkov tubes 1 and 2, not associated with a pulse in the "anti" counter.

---

[9]Richard Madey, A Fast Counting System for High-Energy Particle Measurements. UCRL-1880, October 1954.

[10]Robert Squire, Characteristics of the Production of Neutral Mesons Near Threshold in p-p collisions, UCRL-3137, September 1955.

III. PROCEDURE AND EXPERIMENTAL CONSIDERATIONS

A. Monitor Calibration

The proton flux was measured with an ion chamber, which was calibrated with a Faraday cup. This calibration was repeated for the various energies and at the various beam levels used in the experiment.

B. Beam Energy Measurements

The energy of the cyclotron beam is not a constant, but varies for different operating conditions by as much as 5 Mev. Because the cross section that was to be measured was a sensitive function of the energy, an exact value of the energy was needed. To determine this, two ion chambers were used, between which copper absorbers were placed to trace out the Bragg curve. For our standard of range-energy relations we took the tables of Rich and Madey,[11] UCRL-2301. In addition to the carbon absorbers introduced to degrade the beam energy to desired values, the protons traversed 1.95 g/cm^2 of liquid hydrogen on the average in reaching the sensitive region of the target. This additionally degraded their energy by a few Mev. The resulting energies were:

Run	Lab Angle (degrees)	T (cyclotron) (Mev)	T (bombarding) (Mev)
1	67	342.5	329.0
2	67	333.3	319.5
3	67	327.5	314.5
4	135	342.5	329.0

C. Gamma Telescope Efficiency

The determination of the efficiency of the telescope for the detection of gamma rays of different energies was accomplished in the following manner. First, an experimental test was made of the ability of electrons of various energies to penetrate various thicknesses of lead from 0 to 0.25 in., and

[11] M. Rich and R. Madey, Range-Energy Tables, UCRL-2301, March 1954.

register in scintillator No. 1, scintillator No. 2, and the Cerenkov counter. These electrons were obtained by allowing the bremsstrahlung beam of the Berkeley synchrotron to create a spectrum of electrons in a thin converter, analyzing these electrons in a magnet, and selecting the desired energy. Upon emerging from the magnet, the electrons are caused to pass through an auxiliary electron monitor consisting of two plastic scintillators, each 3/8 in. thick (Fig. 5). In area, these scintillators are 1/9 the area of the 2-by-2-in. lead plate in the main telescope converter position, so as to allow for exploration of various regions of this plate. The number of electrons through the monitor gave the number of electrons incident on the telescope "converter" plate in the area covered by the monitor, and the number of events in which the telescope and the monitor pulses occurred in coincidence was the number of "successful" traversals of the telescope by the monitored electrons. The efficiency for counting electrons is then

$$\text{Eff.} = \frac{\text{No. of coincidences (monitor + telescope)}}{\text{No. in monitor}} \times 100\%.$$

The arrangement of this method, and the electronics employed, are shown in Fig. 5.

Finally, for deriving the efficiency for gamma rays, a numerical integration was performed in which the production of electron-positron pairs by photons was calculated for different depths of the 0.206-in. converter. Then the probability that an electron be produced with an energy E at the depth x in the converter was multiplied by the experimentally derived efficiency for the recording of a count from an electron of energy E that has to penetrate $(0.206-x)$ in. of Pb before entering the telescope.

The results of this determination is indicated in Fig. 6. From the accumulated errors introduced into the problem it is felt that about ± 10% accuracy is a realistic expectation.

D. Background and Subtractions

1. Background

Since the cross section for the reaction studied was quite low, particularly careful attention had to be given to possible sources of background.

There are two essentially different causes of spurious counts in the gamma telescope: multiple accidental coincidences of the kind to cause the electronics to respond as to a gamma ray, and gamma rays having their origin in other than proton-proton collisions.

To eliminate the first kind of background a manifold coincidence requirement was used, parts of which had resolving times of the order of a few millimicroseconds. Experimental checks were made for these accidentals. Blocking the channel in the collimation with lead reduced the counting rate to zero.

The second kind of background might arise from a number of different kinds of events. Admitting the possibility of a "spray" of neutrons from the brass collimation, and of some protons being outside the beam pattern at the telescope entrance window, we consider the following possibilities:

a. π^0 production by neutrons on the air behind the target, in the target walls, the collimation, etc.;

b. π^0 production by stray protons on the target walls, collimation, etc.;

c. π^0 production by protons in the beam on the deuterium "contamination" in the liquid hydrogen;

d. π^0 production by protons multiply scattered from the beam into the target walls;

e. π^- capture in the liquid hydrogen, the π^- mesons coming from protons striking the carbon nuclei in the target entrance windows (the capture[12] leads to $\pi^- + p \rightarrow n + \gamma$ + or $\pi^- + p \rightarrow n + \pi^0$).

A number of other possible sources of background were eliminated by the design of the telescope. Electrons, charged mesons, or protons incident on the array were rejected by the anticounter. Neutrons, by making charge-exchange or ordinary scatterings, could eject protons that could cause counts in Sc 1 and Sc 2, but not in the Cerenkov counter. By capture in lead, neutrons could give 8-Mev gamma rays which could be detected in the Cerenkov counter, but by virture of the approximately 40-Mev threshold of the telescope, these could not cause a count in the Sc 1 - Cer - Sc 2 combination.

The possible sources were dealt with as follows:

a. All neutron-induced events were subtracted by a process outlined below.

---

[12] Panofsky, Aamodt, and Hadley, Phys. Rev. 81, 565 (1951).

b. Stray proton production is similarly subtracted.

c. The normal deuterium content of hydrogen is 1 part in 7000. The contribution from this source was about 0.3%.

d. $\bar{\Theta}^2$ for the scattering of protons by liquid hydrogen in the path length of 50 cm is about 5×10^{-5} (radian)^2. The probability of a proton's scattering into the sensitive region of the target walls is entirely negligible.

e. The surface density of the entrance window of the target is 0.175 g/cm^2, and its composition is essentially C_8H_7. The carbon cross section for π^- production by protons at this energy, at 0°, and within the energy range which would stop within the sensitive hydrogen volume (1.33 g/cm^2), gives a calculated ratio:

$$\frac{\pi^0 \text{ events from } \pi^- \text{ capture}}{\pi^0 \text{ events from p-p production}} \sim 0.2\%.$$

2. Subtractions

The subtraction procedure used was as follows:

Run	Contents of Target	Beam*
A	Liquid hydrogen	deflected*
B	Gaseous hydrogen (STP)	deflected
C	Liquid hydrogen	undeflected*
D	Gaseous hydrogen	undeflected

If one takes the net counting rate as (Run A - Run B) - (Run C - Run D), it can be shown that all the sources of background cancel and the resultant is simply the difference between the yields from protons traversing liquid and gaseous hydrogen, respectively.

*The magnet in the cave could be alternately turned on and off; it was thus possible to steer the proton beam into the target or to allow it to pass, undeflected, beside the target.

IV. EXPERIMENTAL RESULTS

The data, reduced to counts per proton incident on the active target volume and corrected by the subtraction procedure of Section IV-D, are the following:

Run	Lab. Angle (degrees)	Proton Energy (Mev)	Counts per proton x 10^{10}
1	67	329	2.33 ± .10
2	67	319.5	1.36 ± .11
3	67	314.5	1.03 ± .11
4	135	329	0.57 ± .03

V. ANALYSIS OF EXPERIMENT AND INTERPRETATION OF DATA

A. π^0 Meson Decay Spectra

The neutral meson lives about 10^{-15} second and decays into two oppositely directed photons in its own rest frame each of which has an energy equal to half the meson rest mass. When viewed from a frame other than the meson rest frame, these photons may appear with Doppler-shifted energies and with the 180° angle of emission altered by aberration. In this experiment, where the mesons are created near threshold, the meson generally has some velocity with respect to the center-of-momentum frame of the colliding protons. In addition, this c.m. frame is moving in the laboratory system with a velocity dependent upon the initial kinetic energy of the incident proton.

For an isotropic c.m. distribution of neutral mesons, the photon emission (in the c.m. frame) is isotropic, although there is an energy spread whose breadth depends upon meson velocities in the c.m.

If, however, the mesons are emitted in the P state with a $\cos^2\theta$ contribution, there tends to be another kind of photon distribution. Where the meson has zero velocity, the photon distribution must be isotropic, but as the meson velocity increases, the distribution tends to take on some of the $\cos^2\theta$ shape. This can be seen in the limiting case of very high velocities, with β approximately 1, where the aberration of the photons is so great that they appear to go in almost the same direction as the originating meson.

The meson velocities dealt with in this experiment are low, and only a mild modification of the spherical distribution is achieved; nevertheless, it is sufficient to be detectable.

If mesons are created with velocity $\beta_0 C$ in the c.m. system, and with angular distribution $\sum_n a_n P_n(\cos\theta')$ in this system (θ' being the polar angle with respect to the proton beam direction in the c.m. system), then the photon spectrum and angular distribution in the laboratory will be:[10]

$$I(\theta, k, \beta_0)\, d\Omega dk = \frac{1}{\beta_0 \gamma_0 k_0} \sum_n a_n P_n\left(\frac{\cos\theta - \beta}{1 - \beta\cos\theta}\right) \cdot P_n\left(\frac{1}{\beta_0}\left[1 - \frac{k_0}{\gamma_0 \gamma k (1 - \beta\cos\theta)}\right]\right) \cdot \frac{d\Omega dk}{\gamma(1 - \beta\cos\theta)},$$

where:

$\beta_0 C$ = vel. of meson in c.m. frame, and $\gamma_0 = (1 - \beta_0^2)^{-1/2}$,
$k_0 = 1/2\ M_{\pi^0} C^2$,
βC = vel. of c.m. motion in laboratory, and $\gamma = (1 - \beta^2)^{-1/2}$,
θ = angle of photon emission in laboratory with respect to proton beam direction,
$d\Omega$ = observer's solid angle in laboratory,
k = photon energy in laboratory.

It is of course further necessary to know the distributions in the velocity $\beta_0 C$ with which mesons are created in the c.m. frame to obtain the actual photon spectra.

B. Solid Angles and Transmission Factor

The average solid angle subtended by the telescope from the target region was computed as the average of the solid angles subtended from various parts of the target.

Inserted into the collimation channel was an 8-in.-long block of Be. This served to attenuate by dE/dx any charged particles incident upon it. A certain small fraction of the incident gammas was also converted by it and subsequently rejected by the "anticounter." We define a "transmission factor" as the fraction of gammas that get through the Be as well as through one-half the anticounter without conversion. This factor is Tr = 0.85, and is assumed to be independent of the photon energy.

C. Folding Operations and Calculation of Cross Sections

For a given proton bombarding energy, mesons may be created that have energies ranging all the way from zero to some kinematically determined maximum. For the apparatus described here, high-velocity mesons are detected more effectively than low-velocity ones by virtue of the Doppler shifting of the gammas into higher-energy regions where the telescope is a more efficient detector. For this reason, an analysis of the data requires knowledge of the relative numbers of mesons created with different velocities.

The theoretical treatment of meson production as done by Gell-Mann and Watson[2] and by others gives specific predictions for meson energy spectra for the S and P states.

As an example, consider the case where the maximum meson energy is 24 Mev. There are 3 "classes" of meson production contributing to the cross section, each with a different energy spectrum. If we normalize to 1 meson we have for the spectra of kinetic energies in the c.m. system:

$$\text{Class Ss } (\sigma \propto \eta_0^{\,2}): \quad \frac{dn(Ss)}{dT_\pi} = \frac{2}{\pi T_0}\sqrt{\frac{T_\pi}{T_0 - T_\pi}}; \quad T_0 = 24 \text{ Mev};$$

$$\text{Class Pp } (\sigma \propto \eta_0^{\,8}): \quad \frac{dn(Pp)}{dT_\pi} = \frac{128}{3\pi T_0^{\,4}} \cdot T_\pi^{\,3/2}(T_0 - T_\pi)^{3/2}; \quad T_0 = 24 \text{ Mev};$$

$$\text{Class Ps } (\sigma \propto \eta_0^{\,6}): \quad \frac{dn(Ps)}{dT_\pi} = \frac{16}{\pi T_0^{\,3}} \cdot T_\pi^{\,1/2}(T_0 - T_\pi)^{3/2}; \quad T_0 = 24 \text{ Mev}.$$

These three populations are plotted in Fig. 7.

If we write the total meson-production cross section as a function of available pion momentum, in terms of the three contributions, for a particular bombarding energy giving η_0 maximum momentum, we have

$$\sigma(\eta_0) = a_{Ss}\eta_0^{\,2} + a_{Ps}\eta_0^{\,6} + a_{Pp}(C + 1)\eta_0^{\,8},$$

where C is the variable introduced in the Pp angular distribution. The number of counts registered by the telescope, per incident proton, then becomes [10] (assuming the pion energy spectra to be independent of angle):

$$\begin{aligned} C(\eta_0) = N\Delta\Omega\,\mathrm{Tr}\,\Big[& a_{Ss}\eta_0^{\,2}\int_{T_\pi}\int_{k} I_S(T_P, T_\pi, \theta, k)\,\epsilon(k)\,\frac{dn(Ss)}{dT_\pi}\,dk\,dT_\pi + \\ & a_{Ps}\eta_0^{\,6}\int_{T_\pi}\int_{k} I_S(T_P, T_\pi, \theta, k)\,\epsilon(k)\,\frac{dn(Ps)}{dT_\pi}\,dk\,dT_\pi + \\ & a_{Pp}\eta_0^{\,8}\Big\{C\int_{T_\pi}\int_{k} I_S(T_P, T_\pi, \theta, k)\,\epsilon(k)\,\frac{dn(Pp)}{dT_\pi}\,dk\,dT_\pi + \\ & \int_{T_\pi}\int_{k} I_P(T_P, T_\pi, \theta, k)\,\epsilon(k)\,\frac{dn(Pp)}{dT_\pi}\,dk\,dT_\pi\Big\}\Big] \end{aligned}$$

where T_π is integrated from $T_\pi = 0$ to T_π = maximum meson energy (c.m.),

k is integrated from minimum to maximum γ-ray energy (lab),

and N = number of protons/cm^2 for the run in question,

$\Delta\Omega$ = average solid angle for the run in question,

Tr = transmission factor,

$I_S(T_P, T_\pi, \theta, k)$ = spectral intensity of gamma rays in the laboratory system, for the lab viewing angle θ and incident proton energy T_P, resulting from the decay of neutral mesons created with isotropic symmetry and energy T_π in the c.m., normalized to emission of one meson,

$I_P(T_P, T_\pi, \theta, k)$ = same for $\cos^2\theta'$ angular distribution of the neutral mesons in the c.m.,

$\epsilon(k)$ = efficiency for the detection of gammas of energy k by the telescope.

Since there are four experimental points, there are four equations such as this: one for the angle 135°, and one for each of the three different bombarding energies at 67°. If we designate the integrals by F_1 through F_{16}, we can write

$$C_1 = N_1\Delta\Omega_1 \,\mathrm{Tr}\,[a_{Ss}\eta_{01}{}^2F_1 + a_{Ps}\eta_{01}{}^6F_2 + Ca_{Pp}\eta_{01}{}^8F_3 + a_{Pp}\eta_{01}{}^8F_4],$$

$$C_2 = N_1\Delta\Omega_1 \,\mathrm{Tr}\,[a_{Ss}\eta_{02}{}^2F_5 + a_{Ps}\eta_{02}{}^6F_6 + Ca_{Pp}\eta_{02}{}^8F_7 + a_{Pp}\eta_{02}{}^8F_8],$$

$$C_3 = N_1\Delta\Omega_1 \,\mathrm{Tr}\,[a_{Ss}\eta_{03}{}^2F_9 + a_{Ps}\eta_{03}{}^6F_{10} + Ca_{Pp}\eta_{03}{}^8F_{11} + a_{Pp}\eta_{03}{}^8F_{12}],$$

$$C_4 = N_2\Delta\Omega_2 \,\mathrm{Tr}\,[a_{Ss}\eta_{01}{}^2F_{13} + a_{Ps}\eta_{01}{}^6F_{14} + Ca_{Pp}\eta_{01}{}^8F_{15} + a_{Pp}\eta_{01}{}^8F_{16}].$$

The values N_1, $\Delta\Omega_1$, and N_2, $\Delta\Omega_2$ refer respectively to conditions for telescope angles of 67° and 135°.

Because the only unknowns are the a_{Ss}, a_{Ps}, a_{Pp}, and Ca_{Pp}, this is a set of four linear equations in four unknowns. We have solved these by standard methods to arrive at the values given below. The errors that have been attached are from the statistical indeterminancy of the data.

The values are

$$a_{Ss} = 0.020 \pm .010 \text{ mb},$$

$$a_{Ps} = 0.084 \pm .11 \text{ mb};$$

$$Ca_{Pp} = 0.081 \pm .21 \text{ mb};$$
$$a_{Pp} = 0.57 \pm .11 \text{ mb}.$$

Here a_{Ps}, Ca_{Pp} are consistent with zero within the statistical spread shown. Furthermore, the contributions from these terms are small for small values of η_0, and small in comparison with a_{Pp} when η_0 is large. They are included in the statistical spread of the final cross section.

VI. RESULTS

A. Cross Section versus Energy

The total cross section for π^0 production, near threshold, expressed as a function of the kinematic maximum possible meson momentum divided by μc, is a sum of two terms:

$$\sigma_{11}(\text{mb}) = 0.02\,\eta_0^{\,2} + 0.57\eta_0^{\,8}\left\{\begin{array}{l} +\sqrt{(.01\eta_0^{\,2})^2 + (.11\eta_0^{\,6})^2 + (.31\eta_0^{\,8})^2} \\ \\ -\sqrt{(.01\eta_0^{\,2})^2 + (.11\eta_0^{\,8})^2} \end{array}\right.$$

This function is plotted in Fig. 8. The terms $a_{Ps'}$ $Ca_{Pp'}$ are possibly not zero, and serve in this figure to make the two statistical limits unequal.

B. Angular Distribution

The terms with coefficients $a_{Ss'}$ $a_{Ps'}$ Ca_{Pp} contribute mesons having an isotropic distribution, while the term in a_{Pp} contributes mesons having a $\cos^2\theta'$ distribution. Including the possibility that $a_{Ps'}$ Ca_{Pp} are not zero, within the statistical errors attached, we have, for the angular distribution,

$$\frac{d\sigma_{11}(\text{mb})}{d\Omega} = \frac{1}{4\pi}\left[.02\eta_0^{\,2}\left\{\begin{array}{l} +\sqrt{(.01\eta_0^{\,2})^2 + (.11\eta_0^{\,6})^2 + (.21\eta_0^{\,8})} \\ \\ -\ .01\eta_0^{\,2} \end{array}\right\} + \right.$$

$$\left.\frac{3}{4\pi}\ [.57 \pm .11]\ \eta_0^{\,8}\cos^2\theta'\right.$$

If we express this as

$$\frac{d\sigma}{d\Omega} = A + B\cos^2\theta',$$

we can plot the ratio A/B versus η_0. This is done in Fig. 9.

At very low energies, isotropic production dominates. At a value of η_0 of about 0.5 the spherically symmetric and $\cos^2 \theta'$ production are equal, and for higher energies the $\cos^2 \theta$ production rapidly becomes the dominant term.

VII. CONCLUSION

The data presented in this paper indicate that some meson production does occur in the S state,[7] although with a much smaller probability than for production in the P state at all energies except those quite close to threshold. At higher energies, the production is nearly pure P state, and this conclusion is in substantial agreement with other experimental work[6,8] and current theoretical ideas on meson production.

The extreme energy dependence of the cross section at these energies must be modified at much higher energies, and this appears to be the case from the work by Tyapkin et al.[13] Experiments are planned to be done here, when the conversion of the Berkeley cyclotron is completed, that will measure this cross section to a bombarding energy of 730 Mev.

---

[13] Tyapkin, Kosodaev, and Prokoshkin, Doklady Akedemii Nauk USSR 100, No. 4, 689 (1955).

ACKNOWLEDGMENT

The authors wish to thank the Radiation Laboratory for the use of its facilities and the help of its personnel, and in particular, to thank Mr. Vale and the cyclotron operators for their cooperation.

This work was done under the auspices of the U.S. Atomic Energy Commission.

FIGURE CAPTIONS

Fig. 1. Experimental arrangement in the cave area of the cyclotron, with the telescope at the 67° position.

Fig. 2. Liquid hydrogen target.

Fig. 3. Gamma telescope less all shielding.

Fig. 4. Electronics block diagram.

Fig. 5. Experimental arrangement for the determinations of the penetration of electrons through various thicknesses of lead and the counter telescope.

Fig. 6. Efficiency of the telescope for the detection of gamma rays of various energies.

Fig. 7. Probability for a meson to be produced with energy $T_{\pi} \rightarrow T_{\pi} + dT_{\pi}$, where T_0 is the maximum attainable energy, for the three classes of production: Pp, Ps, Ss.

Fig. 8. Cross section for π^0 production in proton-proton collisions as a function of maximum meson momentum in units of μc.

Fig. 9. Ratio of the spherical to $\cos^2 \theta$ contributions to the cross section as a function of η_{θ}.

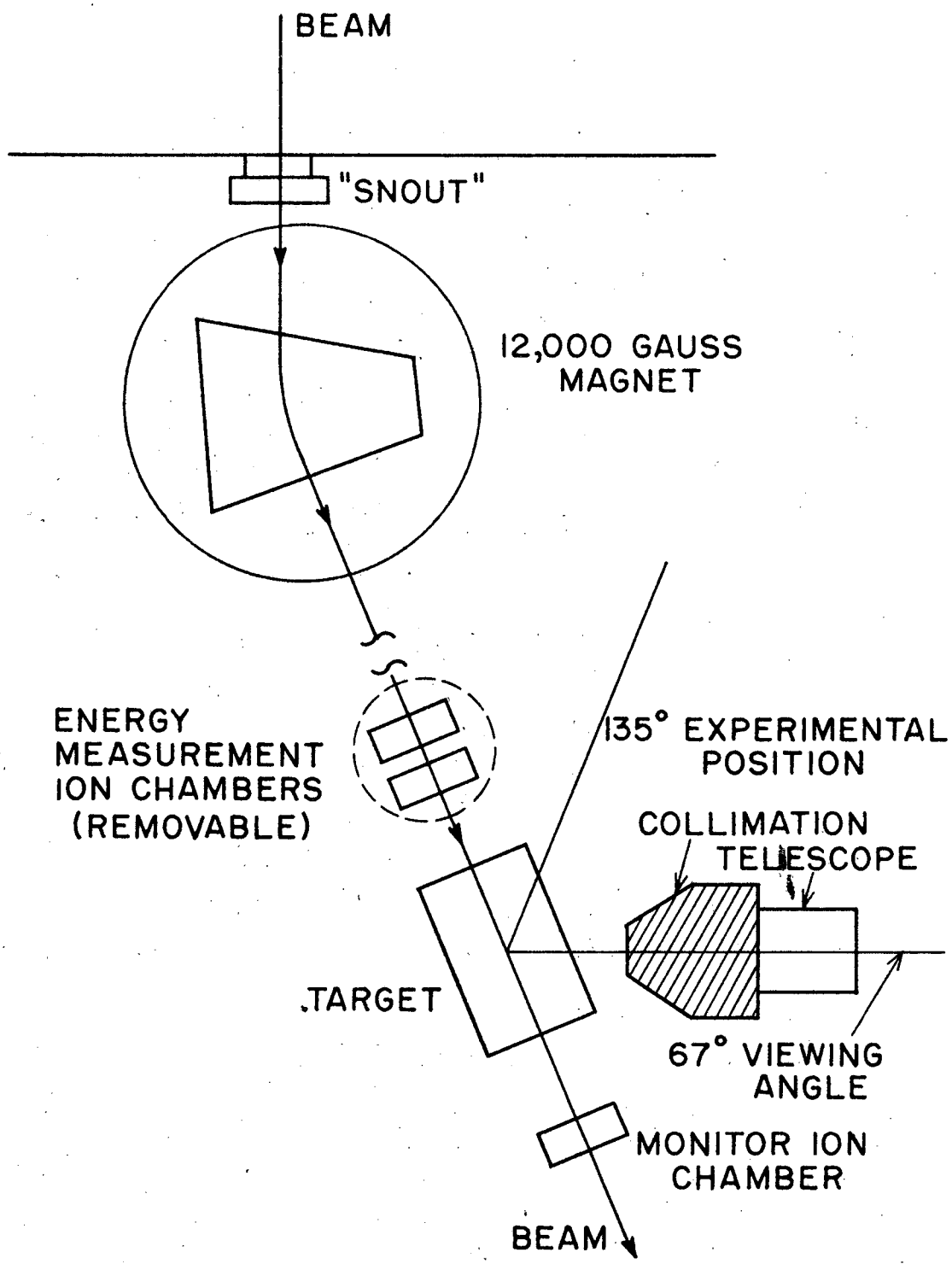
BEAM
"SNOUT"
12,000 GAUSS
MAGNET
ENERGY
MEASUREMENT
ION CHAMBERS
(REMOVABLE)
135° EXPERIMENTAL
POSITION
COLLIMATION
TELESCOPE
TARGET
67° VIEWING
ANGLE
MONITOR ION
CHAMBER
BEAM

24175-1

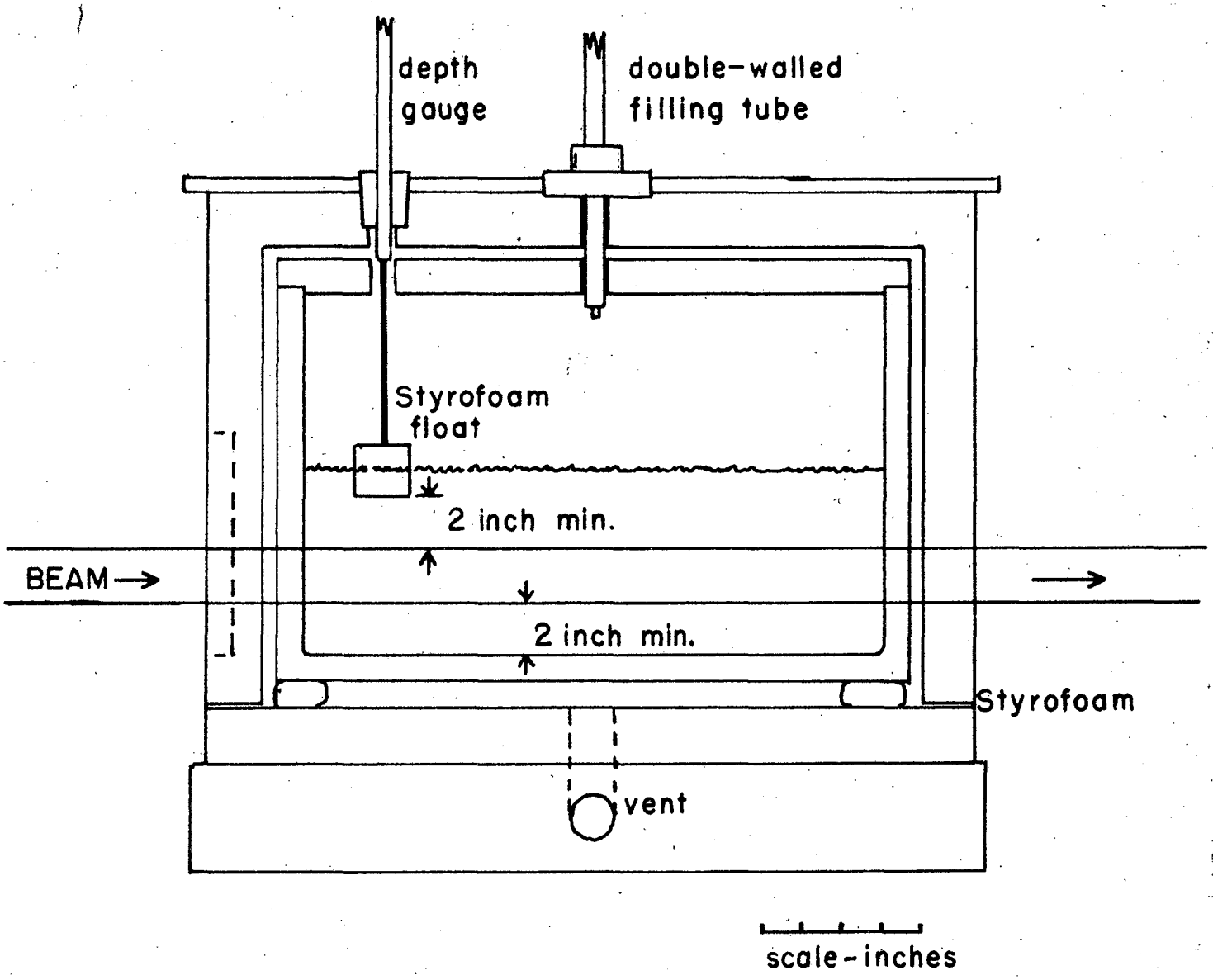
depth
gauge
double-walled
filling tube
Styrofoam
float
2 inch min.
BEAM
2 inch min.
Styrofoam
vent
scale-inches

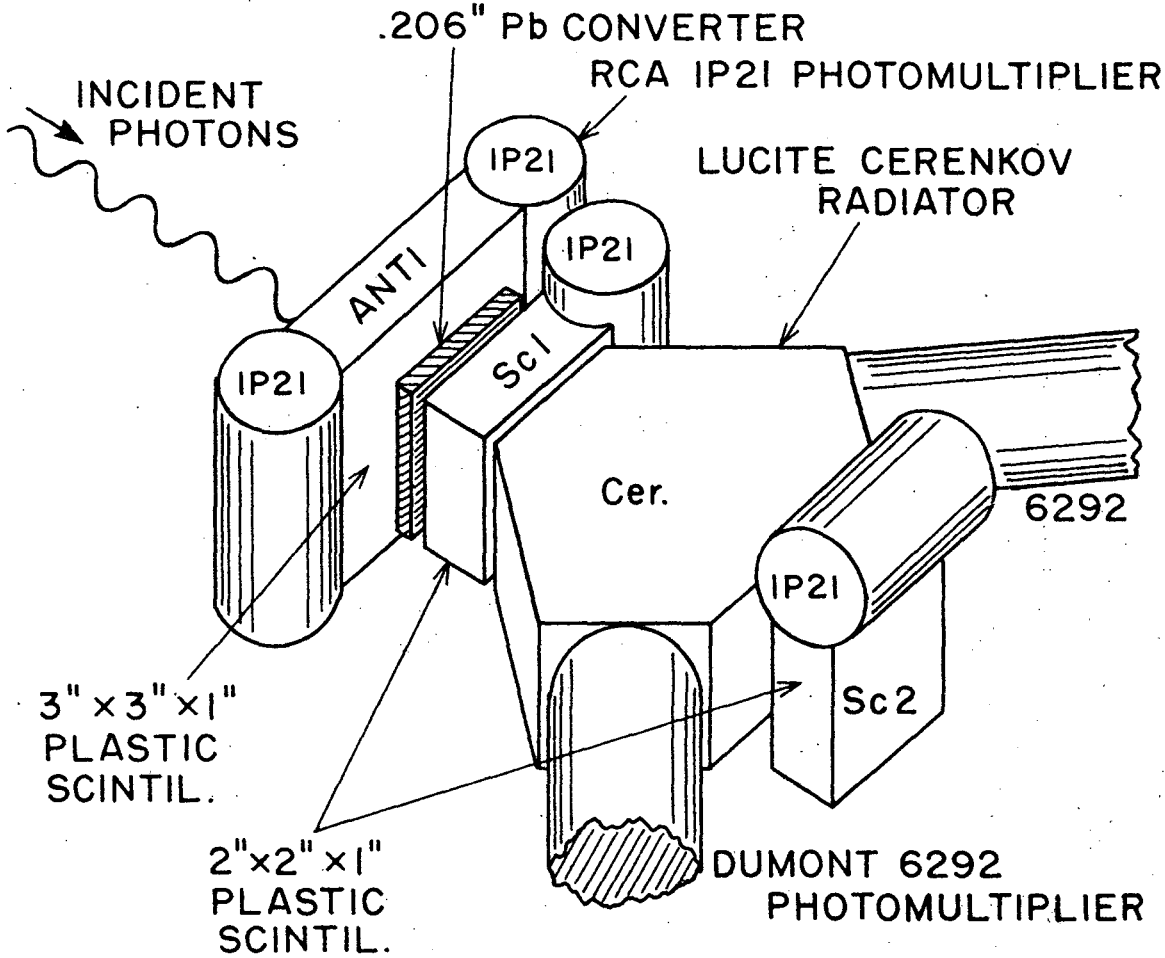
.206" Pb CONVERTER
RCA IP21 PHOTOMULTIPLIER
INCIDENT PHOTONS
IP21
LUCITE CERENKOV RADIATOR
IP21
ANTI
IP21
Sc1
Cer.
6292
IP21
Sc2
3" x 3" x 1" PLASTIC SCINTIL.
2"x2" x1" PLASTIC SCINTIL.
DUMONT 6292 PHOTOMULTIPLIER

24176-1

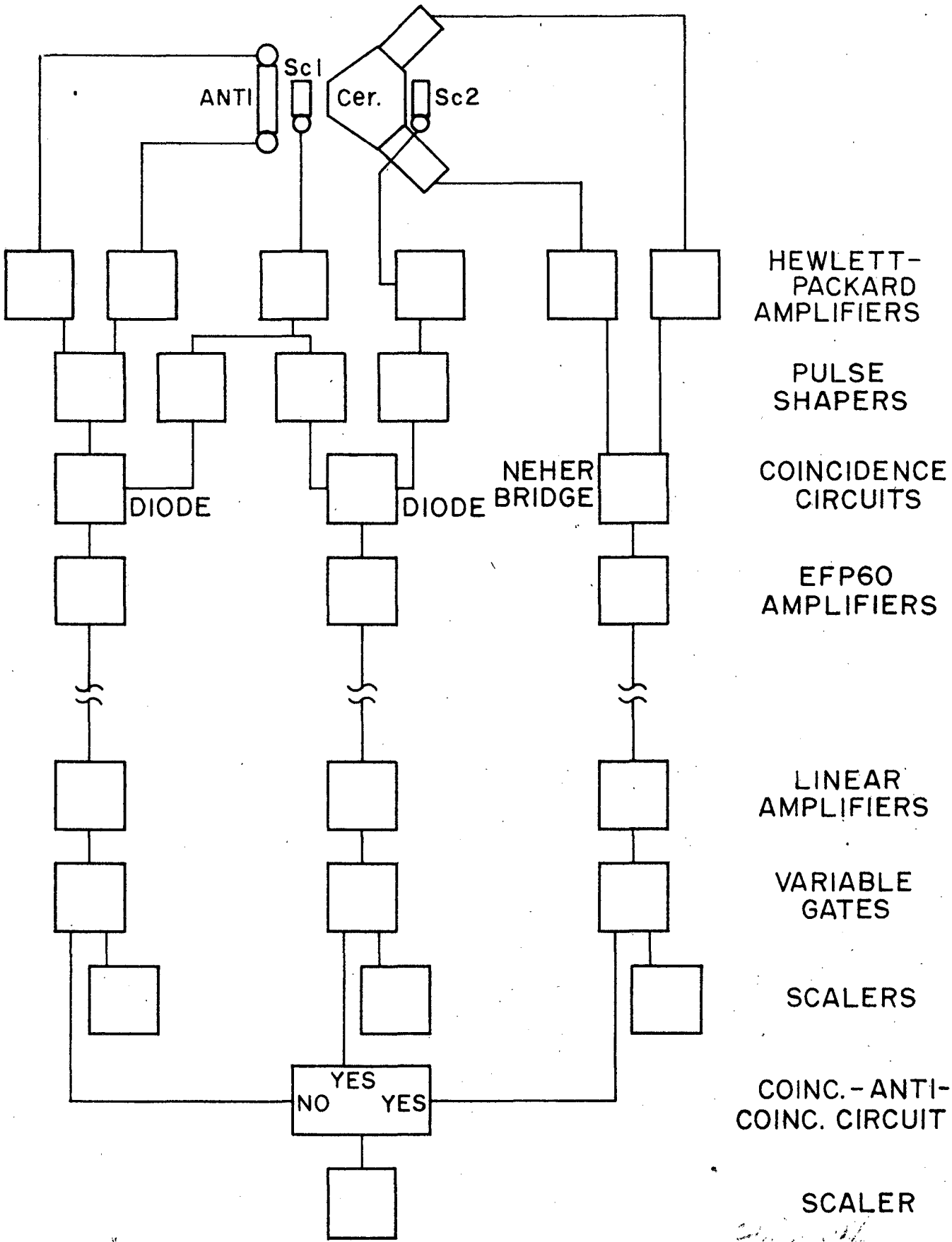
ANTI
Sc1
Cer.
Sc2
HEWLETT-PACKARD AMPLIFIERS
PULSE SHAPERS
DIODE
DIODE
NEHER BRIDGE
COINCIDENCE CIRCUITS
EFP60 AMPLIFIERS
LINEAR AMPLIFIERS
VARIABLE GATES
SCALERS
YES
NO
YES
COINC.-ANTI-COINC. CIRCUIT
SCALER

24177-1

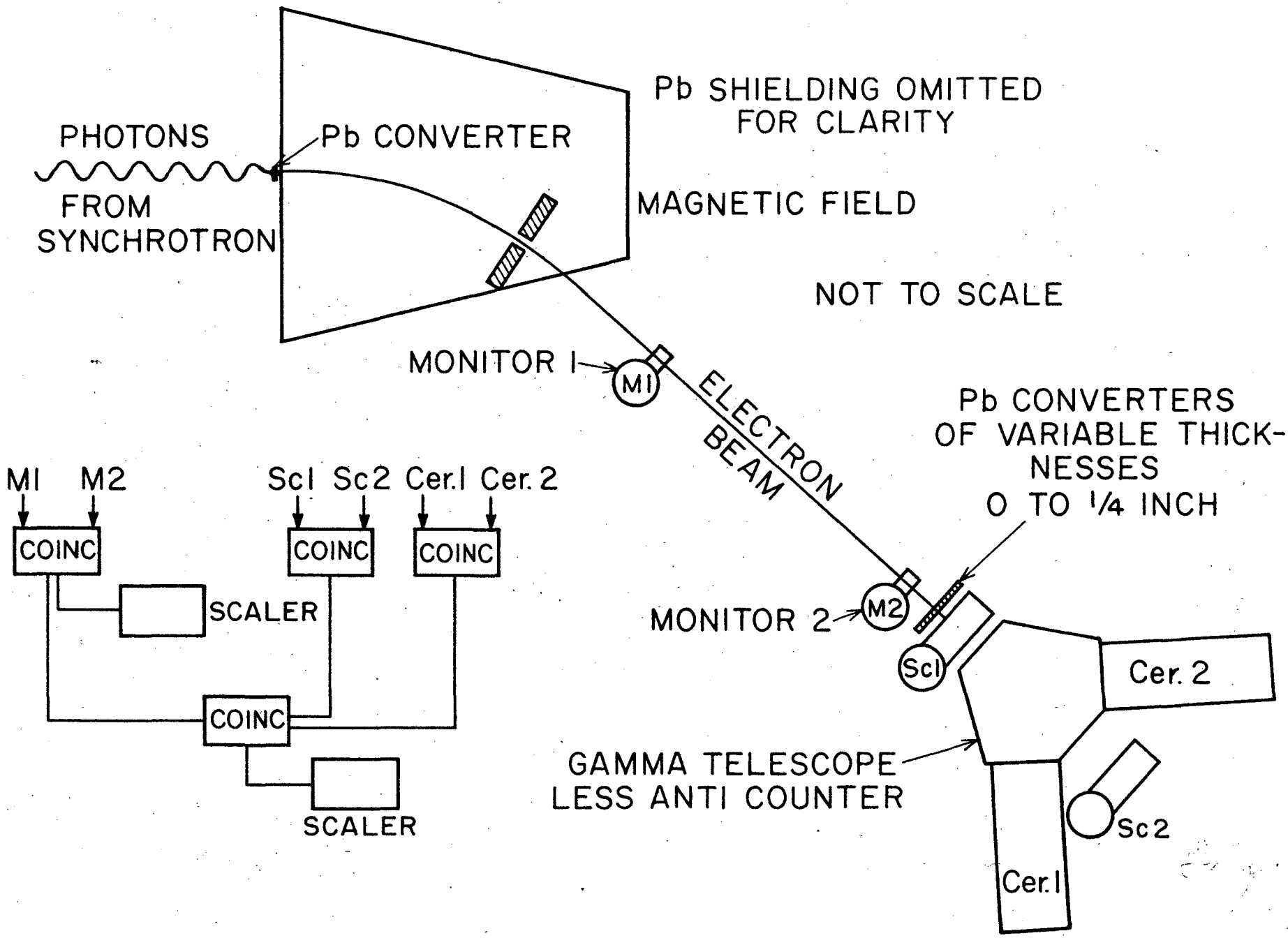
PHOTONS
FROM
SYNCHROTRON
Pb CONVERTER
Pb SHIELDING OMITTED
FOR CLARITY
MAGNETIC FIELD
NOT TO SCALE
MONITOR 1
M1
ELECTRON
BEAM
Pb CONVERTERS
OF VARIABLE THICK-
NESSES
0 TO 1/4 INCH
M1 M2
Sc1 Sc2 Cer.1 Cer. 2
COINC
COINC
COINC
SCALER
COINC
SCALER
MONITOR 2
M2
Sc1
Cer. 2
GAMMA TELESCOPE
LESS ANTI COUNTER
Sc2
Cer.1

24178-1

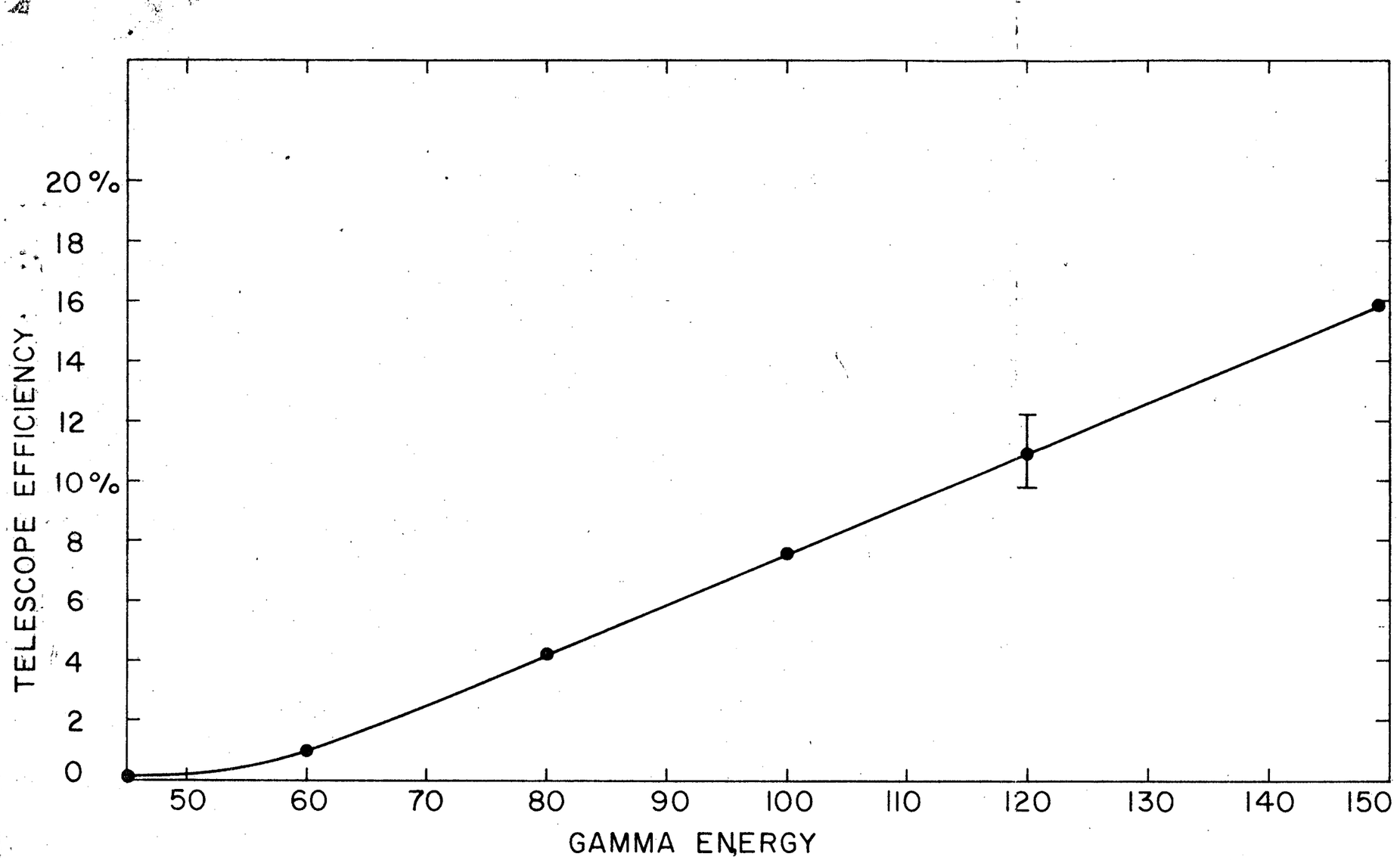
20 %
18
16
14
12
10 %
8
6
4
2
0
TELESCOPE EFFICIENCY
50
60
70
80
90
100
110
120
130
140
150
GAMMA ENERGY

24179-1

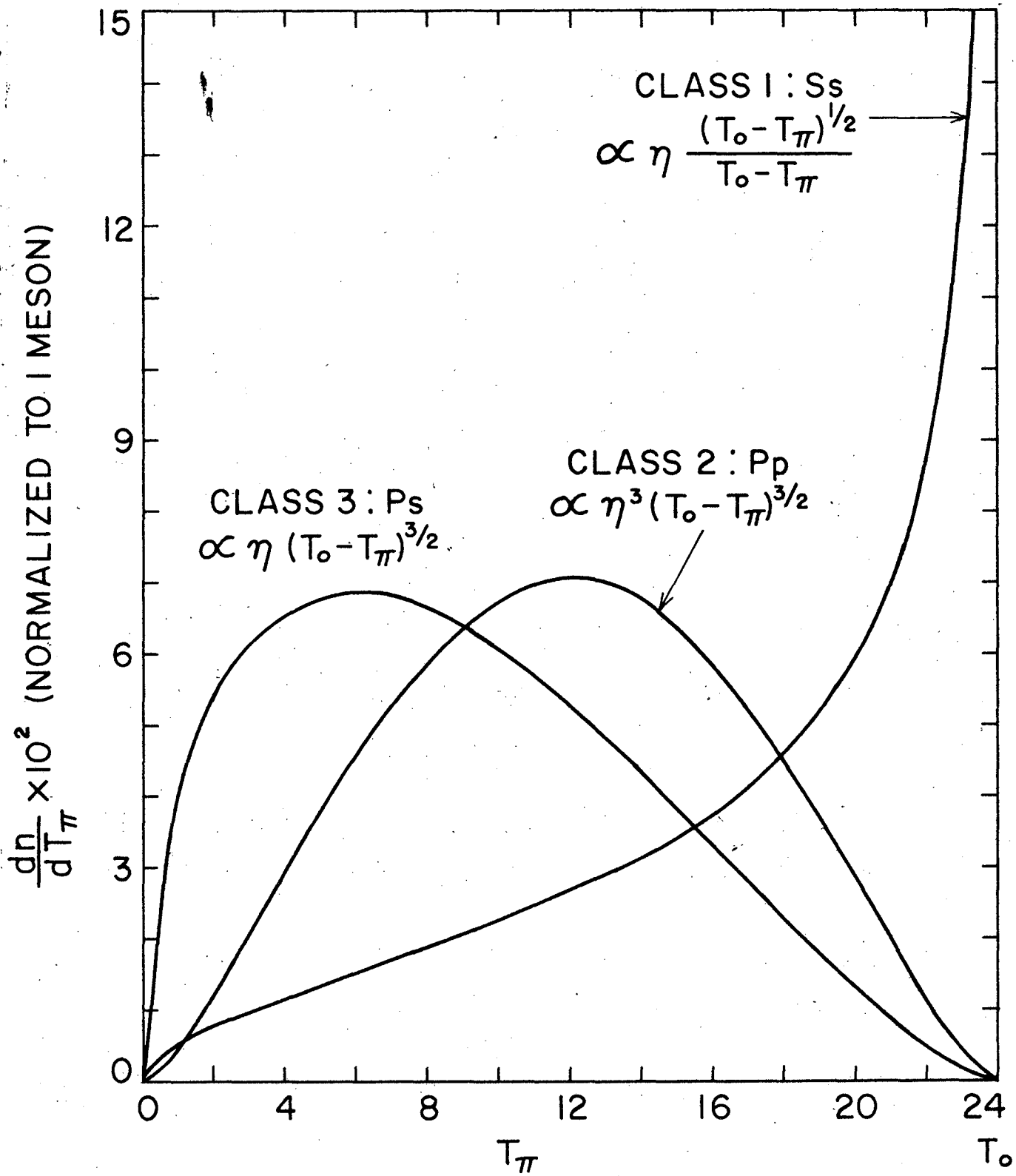
15
12
9
6
3
0
0
4
8
12
16
20
24
T_π
T_o
$\frac{dn}{dT_\pi} \times 10^2$ (NORMALIZED TO 1 MESON)
CLASS 1 : Ss
$\propto \eta \frac{(T_o - T_\pi)^{1/2}}{T_o - T_\pi}$
CLASS 2 : Pp
$\propto \eta^3 (T_o - T_\pi)^{3/2}$
CLASS 3 : Ps
$\propto \eta (T_o - T_\pi)^{3/2}$

24180-1

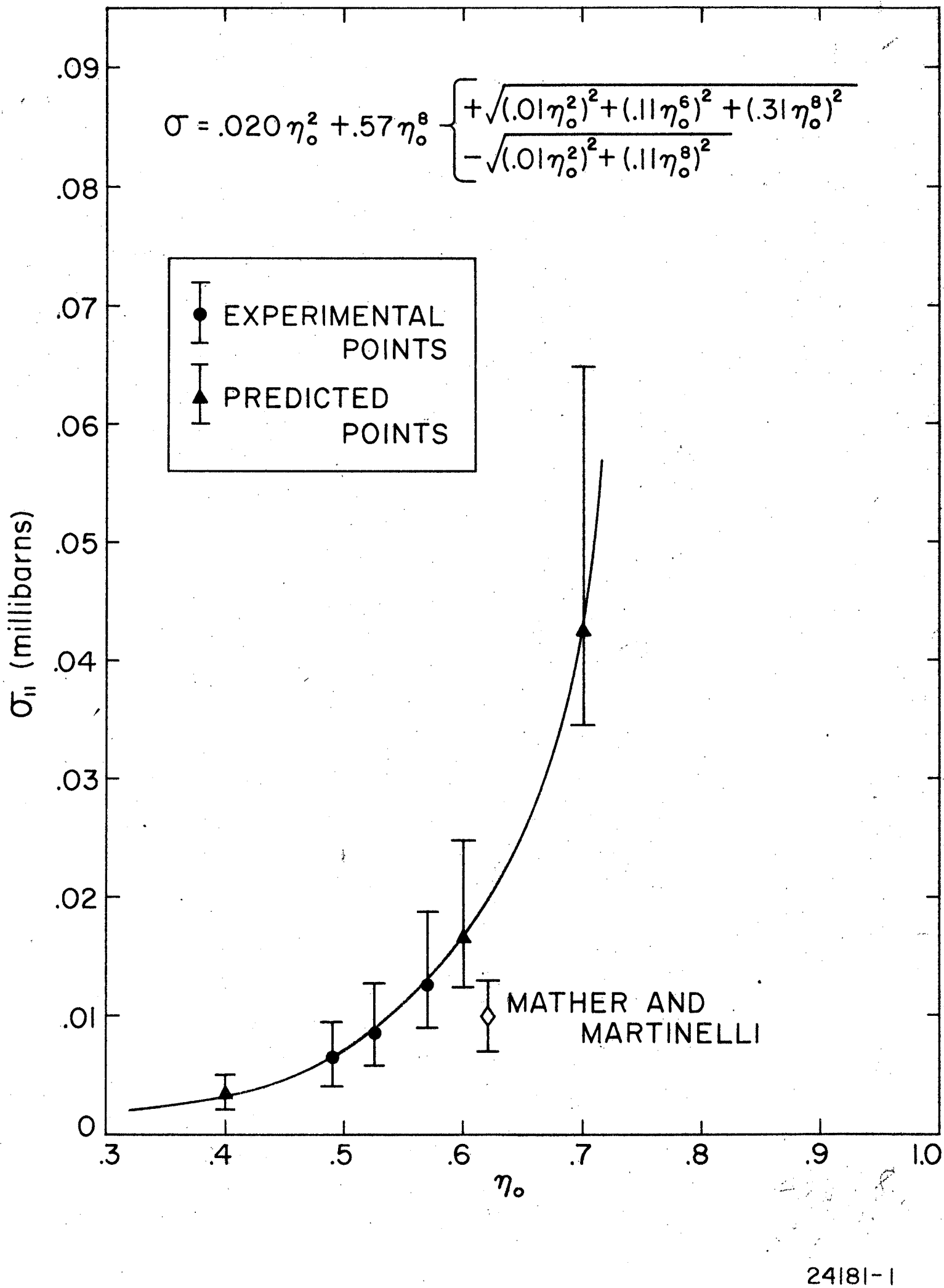
$\sigma = .020\,\eta_o^2 + .57\,\eta_o^8 \begin{cases} +\sqrt{(.01\eta_o^2)^2 + (.11\eta_o^6)^2 + (.31\eta_o^8)^2} \\ -\sqrt{(.01\eta_o^2)^2 + (.11\eta_o^8)^2} \end{cases}$
EXPERIMENTAL POINTS
PREDICTED POINTS
MATHER AND MARTINELLI
σ_{11} (millibarns)
η_o
0
.01
.02
.03
.04
.05
.06
.07
.08
.09
.3
.4
.5
.6
.7
.8
.9
1.0

24181-1

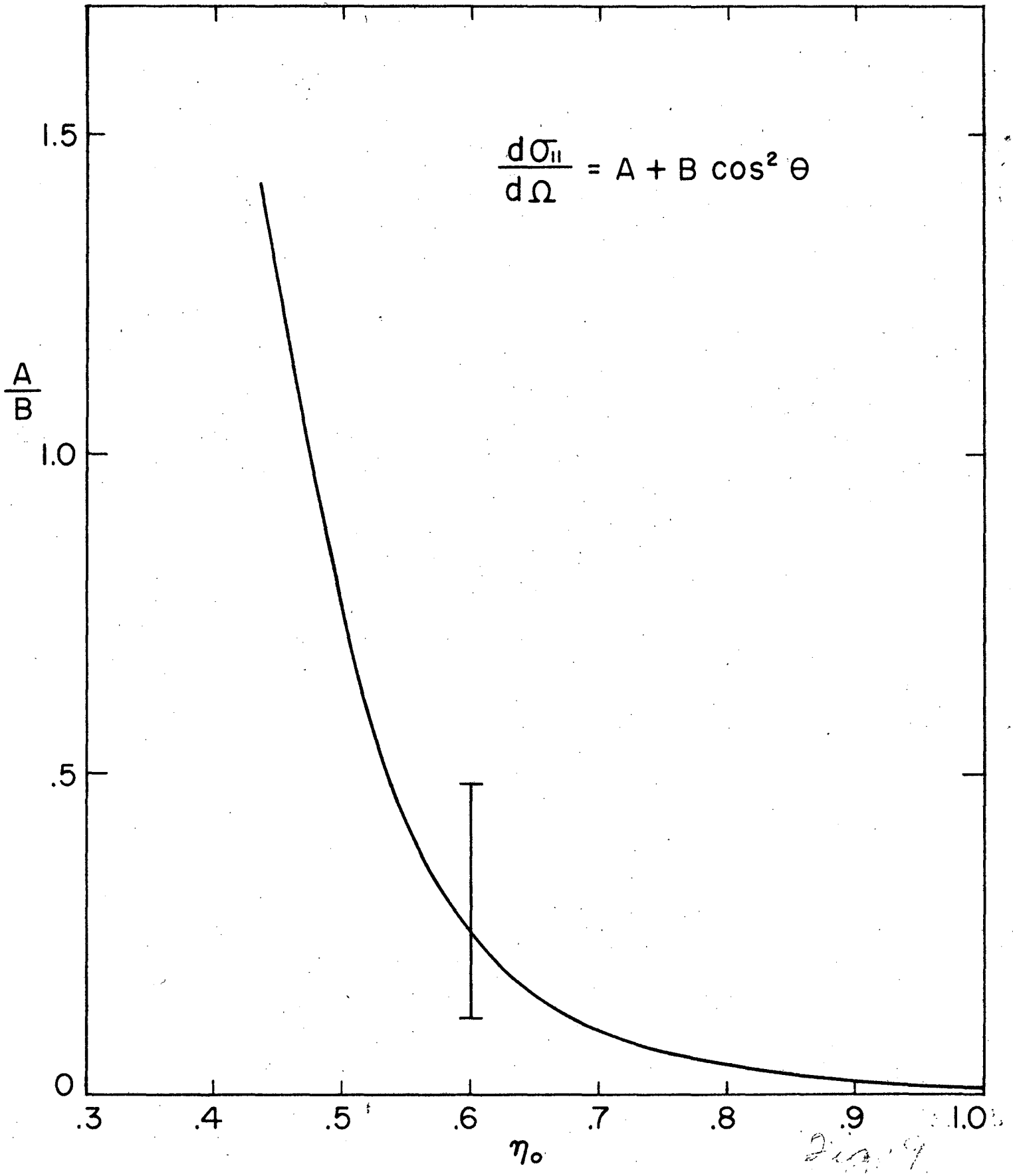
$\frac{d\sigma_{11}}{d\Omega} = A + B\cos^2\theta$
$\frac{A}{B}$
1.5
1.0
.5
0
.3
.4
.5
.6
.7
.8
.9
1.0
η_o

24182-1